ARTICLES

Effects of Pressure and Temperature on the Dynamics of Liquid *tert*-Butyl Alcohol

C. R. Yonker,*,† S. L. Wallen,‡ B. J. Palmer,† and B. C. Garrett†

Environmental and Health Sciences Division, Pacific Northwest National Laboratory,§ Richland, Washington 99352, and Department of Chemistry, University of North Carolina, Chapel Hill, North Carolina 27599

Received: July 2, 1997; In Final Form: September 18, 1997⊗

The solution structure of *tert*-butyl alcohol was investigated as a function of pressure and temperature using high-resolution nuclear magnetic resonance (NMR) spectroscopy. Simulations of the solution structure were undertaken using molecular dynamics and a simple phenomenological model describing clustering in liquid *tert*-butyl alcohol. Chemical shifts, relaxation times (T_1), and line widths (fwhm) of the CH_3 and OH groups were monitored over a pressure and temperature range up to ∼1.0 kbar and from 297 to 423 K, respectively. Simulations demonstrated a cyclic tetramer as the dominant structure in the liquid, with pressure having negligible effects on the overall liquid structure. Temperature shifted the structural distribution and increased the mole fraction of short linear chains in liquid *tert*-butyl alcohol. The rotational correlation time determined from the spin−lattice relaxation time, T_1, and its pressure dependence is consistent with a cyclic structure for liquid *tert*-butyl alcohol that is stable as a function of pressure. This is in contrast to earlier studies of methanol in which pressure was determined to decrease hydrogen bonding and linear chain structures were predominant in the liquid.

Introduction

Aggregation and association in alcohols have typically been used to study hydrogen-bonding dynamics in solutions. *tert*-Butyl alcohol can aggregate through hydrogen bonding, and it has been investigated as both a solid and a liquid using various spectroscopic techniques. NMR has revealed details about the dynamics and hydrogen-bonding behavior of liquid *tert*-butyl alcohol and the interesting structural polymorphism seen in low-temperature solid *tert*-butyl alcohol.[1−5] Temperature is typically the thermodynamic variable used to investigate changes in hydrogen bonding in self-associating molecules such as *tert*-butyl alcohol, but pressure can be used in a similar manner to study the extent of hydrogen bonding. Pressure investigations of butanol have been limited to binary systems of *tert*-butyl alcohol/D_2O by NMR[6] and high-pressure IR studies of the frequency shift in the OH band for 1-butanol.[7] High-pressure NMR investigations of hydrogen-bonding alcohols have provided information about the solution structure in such solvents,[8−13] but they have been limited in number due to the complexity of the experimental system. Consequently, *tert*-butyl alcohol has only been studied at atmospheric pressure as a function of temperature. The main thrust of these earlier investigations was the low-temperature study of the structural polymorphism of solid *tert*-butyl alcohol using NMR.[3,4]

In this investigation, pressure was used to explore the solution structure of *tert*-butyl alcohol at various temperatures and to alter the freezing point for the liquid/solid-phase transition. The chemical shifts of the CH_3 and OH groups of pure *tert*-butyl alcohol were examined over an extended temperature range and pressures up to 0.5 kbar. The observed chemical shifts are sensitive to changes in their local chemical environments, and $\Delta\nu$ the difference between the OH and CH_3 chemical shifts can be used to correlate changes in the hydrogen-bond network of *tert*-butyl alcohol as a function of pressure and temperature. The spin−lattice relaxation times of the methyl groups in *tert*-butyl alcohol were measured as a function of pressure and temperature, and the activation energy for the thermally controlled process of molecular relaxation was determined. Using ^1H NMR measurements, one cannot distinguish among all internal reorientations which contribute to the relaxation of the tetrahedral *tert*-butyl group;[14,15] however, the overall activation energy for *tert*-butyl rotation can be determined. The activation energy for the overall tumbling in liquid *tert*-butyl alcohol has been reported to be ∼38 kJ/mol[3,16] and for *tert*-butyl rotation 37.2 kJ/mol.[3] The activation energy determined in this investigation was lower than the literature values and independent of pressure.

Molecular dynamic simulations were run at the pressure and temperatures corresponding to the experimental conditions. A phenomenological model of aggregation which accounts for the equilibrium between hydrogen-bonded and free (non-hydrogen-bonded) *tert*-butyl alcohol molecules was used to interpret the experimental results relating to the solution structure as a function of pressure and temperature. The goal of this experimental effort was to correlate the molecular simulations with experimental high-pressure NMR results to gain a more fundamental molecular level insight into the structure of liquid *tert*-butyl alcohol and the effect of pressure and temperature on this system.

Experimental Section

Anhydrous *tert*-butyl alcohol (Aldrich Chemical Co., Inc.) was used without further purification or drying. All spectra

* Corresponding author.
† Pacific Northwest National Laboratory.
‡ Department of Chemistry, CB #3290, University of North Carolina.
§ Operated by Battelle Memorial Institute.
⊗ Abstract published in *Advance ACS Abstracts,* November 15, 1997.

S1089-5639(97)02154-3 CCC: $14.00 © 1997 American Chemical Society

were acquired on a Varian (VXR-300) 300 MHz pulsed NMR spectrometer with a 7.04 T superconducting magnet. The high-pressure NMR spectra were obtained without sample spinning, and a spectral resolution between 2 and 4 Hz was maintained over the pressure and temperature range studied. The high-pressure NMR cell utilized in this investigation has been discussed in recent publications.[11,17] The fused silica capillary tubing used in the NMR cell construction was 100 μm i.d. with an external diameter of 360 μm. The spectra were obtained unlocked, which is possible due to the negligible field drift over the course of the experiment. The *tert*-butyl alcohol sample was freeze−pump−thawed 5 times and then loaded into the capillary, after which the capillary was sealed and pressurized. Spin−lattice relaxation times were determined at the experimental temperature and pressure using the standard inversion recovery sequence, $\pi-\tau-\pi/2$. From 8 to 16 variable time delays were used per sample, with a preparation time delay of $>5T_1$ between each inversion recovery pulse sequence. The T_1 values were determined from a nonlinear least-squares fit to the exponential magnetization recovery. For these studies, the pressure was measured using a calibrated pressure transducer (Precise Sensors, Inc.) with a precision of ±0.7 bar. Temperature was controlled to ±0.1 K using the air bath controller on the NMR spectrometer and was calibrated using a reference thermocouple.

Results and Discussion

High-Pressure NMR. The nuclear shielding constant (σ) is an absolute measure of the electronic distribution about the nucleus and its effect on the observed magnetic moment of that nuclei in the applied magnetic field, which is sensitive to a molecule's chemical structure and local solvation environment. The nuclear shielding for a molecule can be related to[18−20]

$$\sigma_{(tert-\text{butyl alcohol})} = \sigma_B + \sigma_A + \sigma_W + \sigma_E + \sigma_{EX} + \sigma_S \quad (1)$$

where σ_B is the contribution from the bulk magnetic susceptibility, σ_A is the contribution from the anisotropy of the magnetic susceptibility for the *tert*-butyl alcohol molecule, σ_W is due to the van der Waals dispersion interactions, σ_E arises from the polarization of the solvent due to a permanent dipole moment in the molecule, σ_{EX} represents the effective short-range exchange interactions, and σ_S is the contribution from specific interactions such as hydrogen bonding.

For the *tert*-butyl alcohol molecule, the CH_3 and OH groups will each experience their own shielding environment as seen from eq 1. The difference between the shielding of the two groups can be related to the specific interactions in solution, σ_S, mainly due to hydrogen bonding of the OH group. The use of the chemical shift difference between the two groups, $\Delta\nu$ (Hz), eliminates the nonspecific contributions that augment the nuclear shielding as a function of pressure and temperature.[11,21] One assumes that changes in pressure or temperature affect these nonspecific contributions in a similar manner for resonances of both groups. Therefore, $\Delta\nu$ can be used to qualitatively estimate changes in the hydrogen-bond network in solution as a function of pressure and temperature.

Figure 1 is a plot of $\Delta\nu$ vs pressure at various temperatures for *tert*-butyl alcohol. As the temperature increases, $\Delta\nu$ decreases at constant pressure. At constant temperature, $\Delta\nu$ increases with increasing pressure. The slope $((\partial\Delta\nu/\partial P)_T)$ also increases with increasing temperature. Similar observations have been reported for methanol and ethanol as a function of pressure.[11,21,22] Hydrogen bonding removes electron density from the vicinity of the nucleus, contributing to the deshielding

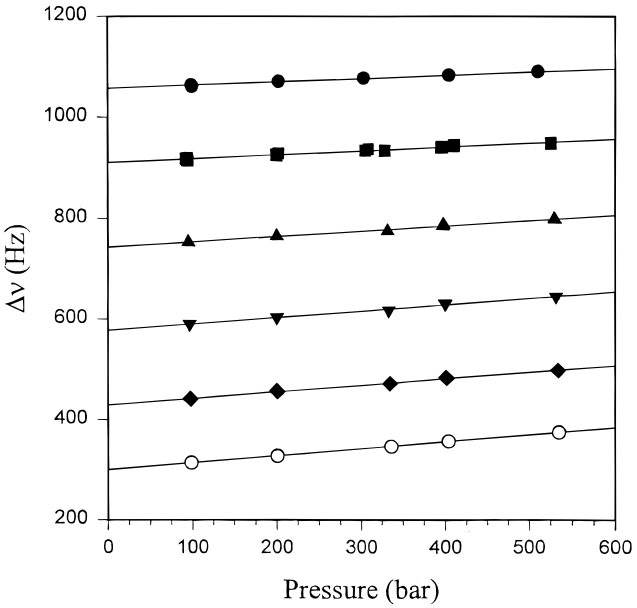

Figure 1. Plot of $\Delta\nu$ (Hz), the difference in the chemical shift between the OH and CH_3 group resonances in *tert*-butyl alcohol, as a function of pressure at (●) 25.0, (■) 50.0, (▲) 75.0, (▼) 100.0, (◆) 125.0, and (○) 150.0 °C, respectively. Solid lines are the least-squares fit to the experimental data.

of the nucleus. Qualitatively, one could state that an increase in $\Delta\nu$ correlates with an increase in the deshielding of the OH proton relative to that of the CH_3 groups. Therefore, this proton exhibits a change in its hydrogen-bonding environment. An increase in $\Delta\nu$ could be related to an increase in the strength of the hydrogen bond or an increase in the extent of hydrogen bonding. The results in Figure 1 demonstrate that increasing temperature tends to decrease the extent of hydrogen bonding in *tert*-butyl alcohol. One would anticipate that increasing temperature would more readily disrupt hydrogen bonds in solution. Increasing pressure at high temperature should have a large effect on the hydrogen-bond network of the solutions contributing to the larger slope $((\partial\Delta\nu/\partial P)_T)$ seen at higher temperatures. The limited pressure range investigated in Figure 1 is due to the low freezing temperature for *tert*-butyl alcohol. As pressure increases at room temperature, *tert*-butyl alcohol solidifies and the signal quality degrades for the solid. We limited the pressure range in our desire to investigate $\Delta\nu$ for the liquid phase. At higher temperatures, we continued to use the same pressure range for self-consistency.

With *tert*-butyl alcohol, as for all liquids, one can freeze the sample by decreasing the temperature or by increasing the pressure. The freezing of neat benzene has been reported by Bull and Jonas as a function of pressure and needs to be considered when using pure solvents with melting points near room temperature, especially in describing their solution dynamics as a function of pressure.[10] One can investigate the change in the freezing point for *tert*-butyl alcohol using high-pressure ^{1}H NMR line widths, $\nu_{1/2}$ (fwhm), as a function of temperature. The results for two different pressures are shown in Figure 2. The narrow ^{1}H resonance of the CH_3 groups in the liquid spectrum broadened significantly during the solid transition. Below its freezing point at 1 bar, 25.4 °C, *tert*-butyl alcohol shows interesting structural polymorphism in the solid phase as a function of temperature as reported in the literature. However, our studies did not investigate this temperature region.[3,4] This investigation focused on freezing points >25.4 °C as a function of pressure. The vertical lines in Figure 2 represent the calculated freezing points from the literature for *tert*-butyl alcohol at the two pressures for which line widths

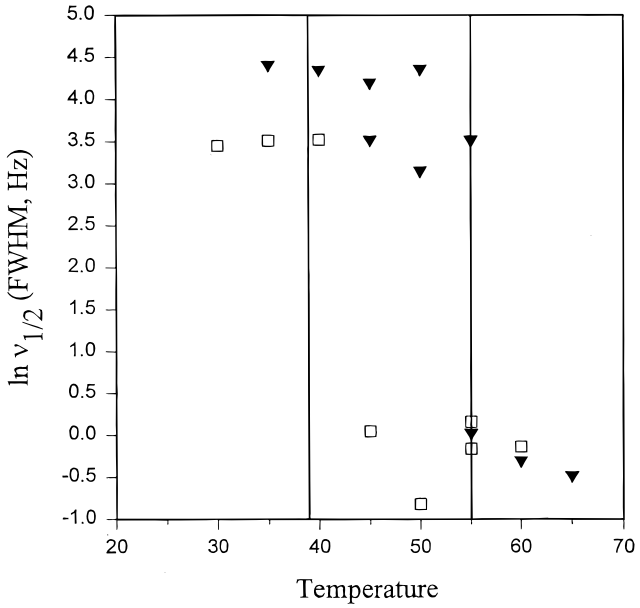

Figure 2. Line widths, ln $\nu_{1/2}$ of ^{1}H CH_3 groups (fwhm in Hz) vs temperature for both liquid and solid phases at (□) 0.41 and (▼) 0.90 kbar, respectively. Vertical lines are calculated freezing points from the literature for *tert*-butyl alcohol at these pressures.[23]

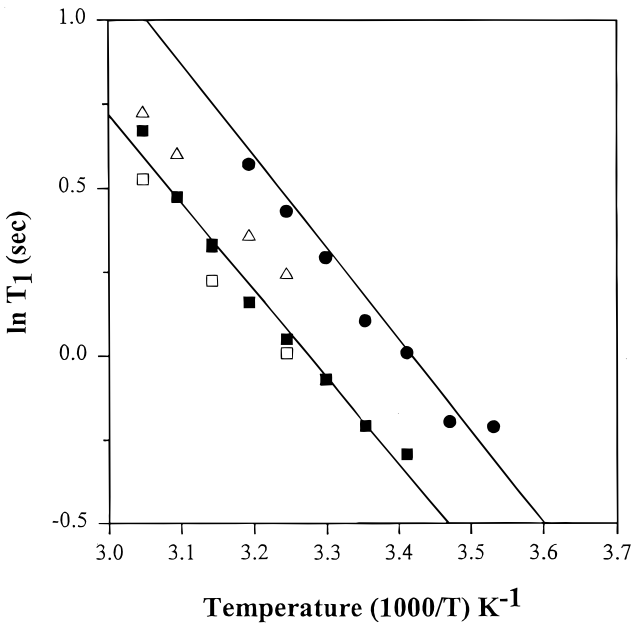

Figure 3. Proton (CH_3) relaxation times (ln T_1) vs reciprocal temperature for both liquid and solid phases at (●) 0.16, (△) 0.46, (■) 0.68, and (□) 1.03 kbar, respectively. Solid lines are the least-squares fit of eqs 7 and 8 to the experimental data.

are shown.[23] The figure clearly demonstrates that the line width can be used to identify the freezing transition in *tert*-butyl alcohol. When the pure sample was rewarmed, the narrow ^{1}H line width was recovered with some hysteresis near the freezing point which most likely was due to the long equilibration time needed for the liquid/solid transition. The proton OH signal in the solid was much broader than the corresponding methyl signal. This is consistent with a shorter effective correlation time for the methyl group due to the ease of internal reorientation in the molecule, for the OH group hydrogen-bonding interactions would have to be broken. It is interesting that high-pressure ^{1}H NMR can determine the phase transition for various thermodynamic conditions in such a facile manner.

The spin−lattice relaxation times, T_1, for the CH_3 groups in *tert*-butyl alcohol as a function of pressure and reciprocal temperature are presented in Figure 3. Our low-pressure (160 bar) measurements match well with the data of Aksnes and Kimtys who have made T_1 studies as a function of temperature at 1 bar.[3] The decrease in T_1 as a function of pressure is similar to the trend reported by Fiorito and Meister for other self-associating liquids.[8] The primary molecular motions contributing to the ^{1}H spin−lattice relaxation for the *tert*-butyl alcohol molecule are from methyl group rotation and the overall tumbling of the molecule. The dipole−dipole interactions which contribute to the relaxation rate of the molecule can be expressed as intramethyl dipole−dipole interactions ($1/T_1^{\text{intra}-CH_3}$) and dipolar coupling between different methyl groups ($1/T_1^{\text{inter}-CH_3}$) on the same molecule. The relaxation time $T_1^{\text{intra}-CH_3}$ is dominated by the rotation of the methyl groups about the C−C bond, while the relaxation time $T_1^{\text{inter}-CH_3}$ is dominated by rotation of the entire *tert*-butyl group. The ^{1}H relaxation rate for *tert*-butyl alcohol is the combination of these relaxation processes.[3,24]

$$1/T_1 = 1/T_1^{\text{intra}-CH_3} + 1/T_1^{\text{inter}-CH_3} \quad (2)$$

where

$$1/T_1^{\text{intra}-CH_3} = (3/20)(\gamma^{4}\hbar^{2}/r^{6})[g(\omega_o,\tau_2) + 3g(\omega_o,\tau_c)] \quad (3)$$

in which r is the distance between the hydrogens in a methyl group (0.179 nm), γ is the magnetogyric ratio for the proton, $\hbar$ is Planck's constant over 2π, and the spectral density function $g(\omega_o,\tau_i)$ is given by

$$g(\omega_o,\tau_i) \equiv [\tau_i/(1 + \omega_o^{2}\tau_i^{2})] + [4\tau_i/(1 + 4\omega_o^{2}\tau_i^{2})] \quad (4)$$

where ω_o is the precessional frequency of the proton in the applied magnetic field. The time constant τ_c appearing in eq 3 is

$$\tau_c^{-1} = \tau_1^{-1} + \tau_2^{-1} \quad (5)$$

where τ_1 is the rotational correlation time of the methyl group and τ_2 is the correlation time for overall tumbling of the *tert*-butyl group. Because τ_1 is very much shorter than τ_2, the correlation time τ_c is expected to be dominated by the methyl group correlation time τ_1. The dipolar interactions between the three methyl groups within the same molecule can be approximated as

$$1/T_1^{\text{inter}-CH_3} = (27/10)(\gamma^{4}\hbar^{2}/r^{*6})g(\omega_o,\tau_2) \quad (6)$$

where r^* is the distance between the centers of the equilateral triangles formed by the hydrogens in the methyl groups (0.311 nm). In the extreme narrowing limit ($\omega_o\tau_c \ll 1$) the spectral density function is simplified and upon substitution in eq 2 the relaxation rate reduces to

$$1/T_1 = (9/4)(\gamma^{4}\hbar^{2}/r^{6})\tau_c + (3/4)(\gamma^{4}\hbar^{2}/r^{6})\tau_2 + 14(\gamma^{4}\hbar^{2}/r^{*6})\tau_2 \quad (7)$$

Because $\tau_2 \gg \tau_1 \sim \tau_c$, eq 7 indicates that the relaxation rate $1/T_1$ will be dominated by τ_2.

Assuming that the molecular motions which contribute to the relaxation of *tert*-butyl alcohol are thermally activated, then the correlation time has the form

$$\tau = \tau_o \exp(E_a/RT) \quad (8)$$

where E_a is the activation energy for the relaxation process. To

TABLE 1: A Comparison of the Activation Energies (E_a) Determined for *tert*-Butyl Alcohol as a Function of Pressure

	E_a		
pressure (kbar)	experimental (kJ/mol)	calculated[a] (kJ/mol)	regressed (kJ/mol)[b]
0.001	38.5[c]	37.9	
	36.9[d]		
0.16	20.4 ± 1.4[e]	38.3	23.2
0.46	20.2 ± 0.4[e]		
0.68	21.7 ± 1.1[e]		22.8
1.03	21.8 ± 2.4[e]		

[a] E_a values calculated using eqs 8 and 9 based on the high-pressure viscosity and molar volume data reported by Matsuo and Makita at 1 and ~200 bar.[25] [b] E_a values determined from the nonlinear regression of eqs 7 and 8 using the experimental T_1 measurements. [c] E_a value reported by Margalit at 1 bar.[16] [d] E_a value reported by Aksnes and Kimtys at 1 bar.[3] [e] E_a values calculated from the slope of T_1 vs reciprocal temperature using eq 8′.

facilitate the comparison of the present experimental data with the extant literature, we have determined the activation energy using three different methods for *tert*-butyl alcohol. First, the activation energies for the relaxation process can be determined from substituting eq 8 for both τ_1 and τ_2 and solving eq 7 using a nonlinear least- squares technique with the experimental relaxation times to solve for the activation energies. However, the activation energies determined in this manner are not well constrained because a proton NMR experiment cannot distinguish between the different internal rotational processes which contribute to relaxation in the *tert*-butyl alcohol molecule. Only the activation energy obtained for τ_2 which should correlate with the overall tumbling of the molecule at two different pressures is presented in Table 1. Second, one can assume that the relaxation process is thermally activated and an equation similar to eq 8 can be used to describe T_1 in this case

$$T_1 = T_1' \exp(-E_a/RT) \tag{8'}$$

Plotting ln T_1 vs $1/T$, one can calculate the activation energy from the slope. These values are reported in Table 1 along with the standard deviation of the slope. Note that the activation energies for τ_2 calculated from the nonlinear least-squares fits and those obtained directly from the slope of ln T_1 vs $1/T$ are nearly the same. This is expected if $1/T_1$ is dominated by the single relaxation time τ_2. Finally, the molecular correlation time can be estimated by the Debye equation

$$\tau = (V/RT)\eta \tag{9}$$

which relates the viscosity (η) and molar volume (V) to the correlation time.[16]

An increase in pressure that increases the bulk viscosity of the solvent will decrease T_1. A pressure increase will also decrease the molar volume of the solvent, but the extent of the decrease (~0.30% over 200 bar at both 30 and 50 °C) is much smaller than the increase in the bulk viscosity seen over the same pressure range at the same temperatures (52% and 39%), respectively.[25] The activation energy estimated from the high-pressure viscosity and molar volume data using eqs 8 and 9 is also included in Table 1. In Figure 3 at a constant temperature, T_1 decreases with increasing pressure which is consistent with arguments based on both bulk and molecular level interpretations of the experimental data. These T_1 values were determined for the CH_3 groups on *tert*-butyl alcohol. An apparent limit is reached at higher pressures due to the increasing incompressibility of *tert*-butyl alcohol under these conditions.

TABLE 2: Molecular Potential Function Parameters for *tert*-Butyl Alcohol; (R_{OH} = 0.945 Å, R_{CO} = 1.43 Å, R_{CC} = 1.53 Å, $\angle_{COH} = \angle_{CCO}$ = 108.5°, $\angle_{CCC}$ = 112°

site	ϵ (kcal/mol)	σ (Å)	q ($\|e\|$)
H	0.0	0.0	0.435
O	0.17	2.97	−0.700
tert-C	0.11	3.80	0.265
CH_3	0.155	3.86	0.0

All the values in Table 1 are in reasonable agreement, but the activation energies determined from the slopes of the high-pressure ^{1}H NMR relaxation time measurements (ln T_1 vs $1/T$ (K^{-1})) do appear to be lower than the values reported by Aksnes and Kimtys and Margalit at 1 bar, which also appear in Table 1.[3,16] The activation energy determined by high-pressure ^{1}H NMR is comparable to that reported for pivalic acid (20.3 kJ/mol) which exists as cyclic dimers.[26] One could postulate from these data that rotational relaxation in *tert*-butyl alcohol is controlled by small cyclic hydrogen-bonded aggregates. There is evidence of cyclic trimers and cyclic dimers in solution studies of alcohol aggregates based on ^{1}H chemical shift measurements as a function of concentration.[27−29] It is interesting to note that pressure does not affect the activation energies, either those measured experimentally or calculated based on the high-pressure viscosity data. This implies that the geometry of the aggregate must be able to achieve reasonably free rotation about the C−O bond axis even as the density (number of molecules) increases. A cyclic hydrogen-bond structure could permit this type of free molecular rotation.[29]

Molecular Dynamic Simulations and Equilibrium Cluster Model. Simulations were performed on *tert*-butyl alcohol using a rigid model that treated the methyl groups as combined atoms. Because very little data was available on the pressure−temperature−density behavior of *tert*-butyl alcohol, except near standard conditions, it was necessary to run the simulations using a constant pressure algorithm. Unfortunately, most molecular models do an extremely poor job of reproducing the experimental pressure at a given temperature and density so it was necessary to recalibrate the parameters in the molecular potential function for *tert*-butyl alcohol to at least reproduce the pressure−temperature−density behavior near standard conditions. Starting with Jorgensen's OPLS potential for *tert*-butyl alcohol,[30,31] the parameters were systematically varied until reasonable agreement was found between the pressure calculated during a molecular dynamics simulation and the experimental pressure at the same conditions of temperature and density. An effort was also made to simultaneously match the experimental value of the enthalpy of vaporization.

The intermolecular interactions between different sites on *tert*-butyl alcohol are described by a combination of Lennard-Jones and Coulomb interactions of the form

$$\phi_{ij}(r_{ij}) = 4\epsilon_{ij}\left[\left(\frac{\sigma_{ij}}{r_{ij}}\right)^{12} - \left(\frac{\sigma_{ij}}{r_{ij}}\right)^{6}\right] + \frac{q_i q_j}{r_{ij}} + a_{ij} + b_{ij}(r_{ij} - r_c) \tag{10}$$

If $r_{ij} > r_c$, then the interaction vanishes. The parameters a_{ij} and b_{ij} are chosen so that both the potential and the force vanish at the cutoff distance r_c. The value of the cutoff was set at 9.5 Å. For the OPLS model, each atom A is assigned a well depth ϵ_A, a hard sphere radius σ_A, and a partial charge q_A. The parameters in the potential are then calculated from the combining rules $\epsilon_{AB} = (\epsilon_A\epsilon_B)^{1/2}$ and $\sigma_{AB} = (\sigma_A + \sigma_B)/2$. The final parameters used for the simulations described here are listed in Table 2. The dihedral potential for rotations about the CO bond is given by Jorgensen.[30] From a short simulation at

300.65 K and a density of 0.778 g/cm^3, the model gave a pressure of −11.2 bar, compared to the experimental value of ∼1 bar.[32] The enthalpy of vaporization, estimated from the formula[33]

$$\Delta H_{vap} = RT - U_l - P_l V_l \qquad (11)$$

where U_l is the internal energy of the liquid, was 9.2 kcal/mol. This value is substantially below the experimental value of about 11 kcal/mol.[32] Because the agreement between the model and the experimental properties of *tert*-butyl alcohol is marginal, the results reported are expected to give only qualitative insights into the behavior of *tert*-butyl alcohol over the range of temperatures and pressures studied.

Using this model, simulations were run at the temperature−pressure points of (323 K, 95.1 bar), (323 K, 532.9 bar), (423 K, 100.0 bar), and (423 K, 542.6 bar). The temperature and pressure were maintained using the Andersen−Nosé constant pressure−constant temperature algorithm.[34,35] The rigid bond and angle constraints were maintained using a variant of the SHAKE algorithm, and the equations of motion were integrated using the velocity Verlet algorithm recast as a Gear 3-point predictor−corrector.[36] Each simulation was run for a total of 50 ps using a 1.25 fs time step.

The simulations were used to analyze hydrogen-bonding patterns in *tert*-butyl alcohol. A hydrogen bond was defined to have formed between two *tert*-butyl alcohol molecules if the alcohol proton on one molecule was within 2.5 Å of the oxygen on the other molecule. The distance 2.5 Å corresponds to the location of the minimum after the first peak in the pair distribution function between the oxygens and the alcohol protons. Using this definition of a hydrogen bond, the configurations generated by the simulation were broken up into clusters of hydrogen-bonded *tert*-butyl alcohol molecules. The clusters were chosen by requiring that each molecule in a cluster be hydrogen bonded to at least one other molecule in the cluster. Each cluster was then further analyzed to determine the number of alcohol protons that were not participating in a hydrogen bond. If there were no free protons, then the cluster was assumed to be forming a ring structure; if the cluster had one or more free protons, then the cluster was assumed to be forming a chain or branched chain structure. The result of this analysis was the mole fraction of molecules located in rings of size N, r_N, and the mole fraction of molecules located in chains of size N, c_N, where N represents the number of molecules in a cluster. The results of these analyses for the four simulations are shown in Figure 4. All four simulations show a sharp peak in the distribution of rings centered at four molecules. The r_N then decay rapidly with increasing N. The distribution of chains is fairly broad and flat for the two simulations at 323 K, and most of the clusters are forming rings with four to six molecules. At higher temperatures, however, a significant number of short, hydrogen-bonded chains also form. While the distributions appear to be sensitive functions of temperature, the effect of pressure is much less pronounced. The fact that most of the clusters are forming rings in *tert*-butyl alcohol contrasts the behavior observed in simulations of methanol. For methanol, almost all the clusters were hydrogen-bonded chains.[11]

The picture of *tert*-butyl alcohol forming only small rings is reinforced by the pair distribution function between the alcohol hydrogen and the oxygen atom. The pair distribution function calculated from the simulation at 323 K and 95.1 bar is shown in Figure 5. The distribution function shows a sharp peak centered at 1.7 Å, corresponding to hydrogen bonding, and another broad peak centered at 3 Å. The second peak corresponds to the OH distance across the small hydrogen-bonded ring. The second peak is followed by a broad exclusion zone from between 4 and 7 Å. The small rings would be oriented so that the methyl groups point out from the ring, effectively screening the ring from interacting with other OH groups, resulting in a low value for the pair distribution function in this range.

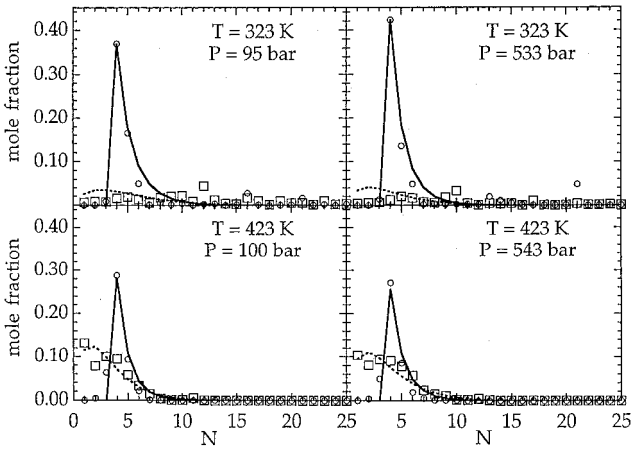

Figure 4. Molecular dynamic simulations and equilibrium cluster model of *tert*-butyl alcohol as a function of pressure and temperature. Mole fraction of ring (○) and chain (□) structure vs cluster size (N) at the noted temperatures and pressures. The symbols represent the MD simulations and the solid and dotted lines represent the equilibrium cluster model fit to the ring and chain distributions.

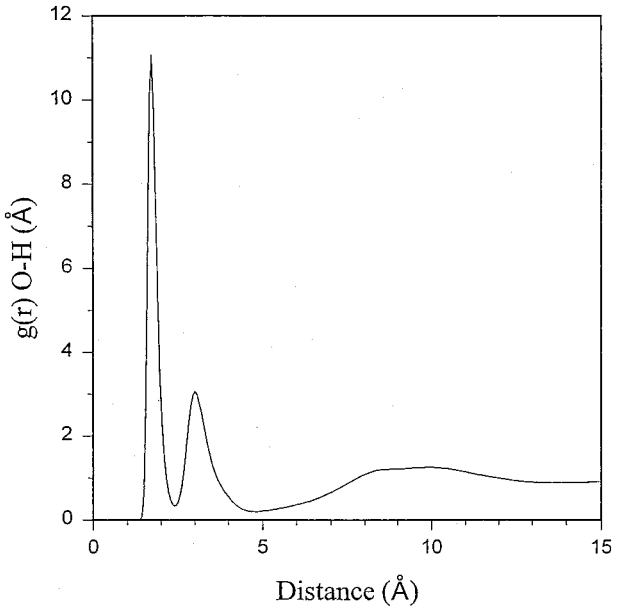

Figure 5. Plot of the pair distribution function ($g(r)$ O−H) as a function of distance calculated from the molecular dynamics simulation for *tert*-butyl alcohol at 323 K and 95.1 bar.

To model the distributions of rings and chains, a simple one-dimensional aggregation model[37] used previously to model hydrogen-bonded chains in methanol[11] was generalized to include the rings. This model is almost identical with one developed by Jacobsen and Stockmeyer to study ring−chain equilibria in polymer solutions.[38] The original aggregation model derived the equilibrium constant

$$K = \exp[-N(\mu_N^0 - \mu_1^0)/k_B T] \qquad (12)$$

between N monomers and a chain of length N by using the fact that chains of different lengths in an equilibrium distribution must all be at the same chemical potential. The free energy

per monomer in a cluster of size N is μ_N^0 and μ_1^0 is the free energy of an isolated monomer in the system. If c_N is the mole fraction of molecules that are in chains of size N, it follows that c_N can be written as

$$c_N = Nc_1^N \exp[-N\mu_N^0/k_BT] \tag{13}$$

For linear aggregates, it was further assumed that

$$N\mu_N^0 = -(N-1)\alpha k_BT \tag{14}$$

where α is a number that is independent of N. This formula assumes that the free energy for forming a hydrogen bond is the same for different size clusters. The factor of $N-1$ on the right-hand side comes from the fact that there are $N-1$ hydrogen bonds in a chain of N monomers. Solving for α and substituting the result back into the expression for c_N gives

$$c_N = Nc_1^N e^{\alpha N-\alpha} \tag{15}$$

The value of c_1 for a given value of α can be found from the normalization condition

$$\sum_{N=1}^{\infty} c_N = 1 \tag{16}$$

To generalize the model to include rings, it is necessary to consider (i) the change in the number of hydrogen bonds that occurs when a chain forms a ring, (ii) the decrease in entropy caused by tying the two free ends of a chain into a ring, and (iii) the steric factors that prevent the formation of very small rings. The change in the number of hydrogen bonds is trivially incorporated by noting that a ring of N monomers has N hydrogen bonds compared to the $N-1$ hydrogen bonds for the same size chain.

The effect of closing the chain into a ring can be included into the model by making use of a result from Jacobson and Stockmeyer.[38] They calculated that the equilibrium constant between a system containing a chain of length M and a ring of size N and a system containing a chain of size $M+N$ was of the form

$$\frac{c_M r_N}{c_{M+N}} = BN^{-5/2} \tag{17}$$

where B is a constant independent of M and N. This formula assumes that the energy of forming a hydrogen bond is the same for both rings and chains and that the statistical properties of the chain are Gaussian. It follows that the distribution r_N is

$$r_N = BN^{-3/2}c_1^N e^{N\alpha} \tag{18}$$

Finally, the effect of steric strain on small rings can be included by assuming that the strain energy for rings less than some size N_0 is great enough so that no rings form and the distribution r_N is essentially zero. For ring sizes greater than or equal to N_0, the strain energy is zero and the free energy for forming a hydrogen bond in a ring is the same as for forming a hydrogen bond in a chain. This assumption can then be incorporated into the normalization condition

$$\sum_{N=1}^{\infty} c_N + \sum_{N=N_0}^{\infty} r_N = 1 \tag{19}$$

For a given value of α and B, this equation can be solved for c_1, which can then be used to evaluate the remaining c_N and r_N. Although the normalization condition cannot be solved analytically, it is straightforward to find c_1 numerically.

TABLE 3: Parameters Obtained from the Aggregation Model for *tert*-Butyl Alcohol

simulation	T (K)	P (bar)	α	B	ρ (g/cm^3)
1	323	95.1	3.27	14.1	0.749
2	323	532.9	2.88	24.6	0.810
3	423	100.0	1.53	27.7	0.588
4	423	542.6	1.81	17.7	0.714

This model was used to fit the distributions c_N and r_N calculated from the simulations. The value of N_0 was set equal to four. The fitted distributions are also shown in Figure 4, along with distributions obtained from the simulations. The parameters α and B derived from the fits are summarized in Table 3. The densities, ρ, calculated from the simulations are also included. The parameter B does not exhibit any consistent behavior as a function of temperature and pressure, although all the values of B appear to be in the neighborhood of 20. The α parameter does not behave consistently as a function of pressure, but does show a consistent drop as the temperature is increased. Part of the temperature dependence comes from the fact that α can be written as

$$\alpha = -\frac{\Delta G_{HB}}{k_BT} \tag{20}$$

where ΔG_{HB} is the free energy for forming a hydrogen bond. The factor of T in the denominator accounts for about half of the drop in α on going to higher temperatures. The remainder can be accounted for by writing ΔG_{HB} as

$$\Delta G_{HB} = \Delta H_{HB} - T\Delta S_{HB} \tag{21}$$

where ΔH_{HB} and ΔS_{HB} are the enthalpy and entropy of forming a hydrogen bond. Previous studies on methanol showed that both ΔH_{HB} and ΔS_{HB} were negative and relatively insensitive functions of density. If the same remains true for *tert*-butyl alcohol, then $-\Delta G_{HB}$ would decrease with increasing temperature. However, the fact that both α and B appear to depend on temperature and pressure suggests that fitting the chemical shifts to a detailed aggregation model similar to that reported previously for methanol[11] is not feasible.

The simulations generally support the idea that liquid *tert*-butyl alcohol is dominated by the presence of small, hydrogen-bonded rings of molecules. The distributions show only a small number of chains at lower temperatures, but a significant number of short chains appear at higher temperatures. The effect of pressure on the distributions appears to be much smaller over the range of pressures examined. The shift from rings to chains is consistent with the changes in $\Delta\nu$, because the appearance of more chains corresponds to a relatively large increase in the number of non-hydrogen-bonded hydrogens in the system.

Conclusions

This effort is the first high-pressure study of *tert*-butyl alcohol investigating the effects of pressure and temperature on solution structure for this molecule. Changes in the chemical shift ($\Delta\nu$) with pressure were larger at higher temperatures but smaller than shifts seen in $\Delta\nu$ values as a function of temperature. Linewidth studies of *tert*-butyl alcohol as a function of pressure demonstrated that these are a sensitive determinant of the change in the freezing point of the neat solvent as pressure increases. As the phase-transition temperature increased with pressure, the line width of the ^{1}H resonance for the CH_3 group followed suit

on going from a liquid to the solid. Over this same pressure range, the ^{1}H resonance of the OH group broadened and decreased as the liquid *tert*-butyl alcohol solidified. Some hysteresis was seen for the transition point which was due to the slow equilibrium process at the solid/liquid phase transition. The peak-width behavior for the OH group is most likely due to the hydrogen bonding of this group increasing the relaxation rate of the proton, which broadens the NMR signal.

Results from the high-pressure NMR investigation of *tert*-butyl alcohol demonstrate that $\Delta\nu$ is dominated by temperature effects which reflect the extent of the hydrogen-bond network through an apparent decrease in hydrogen bonding with increasing temperature. The relaxation times shown as a function of pressure and temperature in Figure 3 qualitatively follow the $\Delta\nu$ results for *tert*-butyl alcohol. At higher temperatures, the hydrogen-bonding network (density) decreases and the relaxation time would be expected to increase. At constant temperature, as pressure increases the hydrogen-bond network (density) should increase and the relaxation time should decrease accordingly. Simulations of cluster equilibrium as a function of pressure and temperature illustrate the role of temperature in decreasing the mole fraction of cyclic clusters and increasing the number of free protons, while pressure appears to have a negligible effect over the range investigated. The lack of a pressure dependence on the activation energy determined from the T_1 measurements appears to support the molecular dynamics simulations in which the aggregates in solution are dominated by cyclic tetramers. Joarder et al. have reported cyclic hexamers in liquid *tert*-butyl alcohol.[39] While in Figure 4 our simulations show a small mole fraction of cyclic hexamers, it is clear that the dominant form is a cyclic tetramer. However, Joarder's analysis did not consider the possibility of cyclic structures other than hexamers.

Analysis of the T_1 values does not give any detailed information on cluster size, but does reveal that the activation energy is relatively insensitive to pressure. This is consistent with the results of the molecular dynamics simulations, which suggest that the distributions of chains and cyclic *n*-mers are also insensitive to pressure and that the environment of the *tert*-butyl alcohol molecules does not change drastically as pressure is increased. The overall combination of high-pressure NMR with molecular dynamic simulations of the solution structure of neat *tert*-butyl alcohol gives one a better understanding of the role of temperature and pressure on the solution physics and hydrogen bonding of this molecule.

Acknowledgment. Work at the Pacific Northwest National Laboratory (PNNL) was supported by the Office of Energy Research, Office of Basic Energy Sciences, Chemical Sciences Division of the U.S. Department of Energy, under Contract DE-AC076RLO 1830.

References and Notes

(1) Sweeting, L. M.; Becker, E. D. *J. Phys. Chem.* **1984**, *88*, 6075.
(2) Tucker, E. E.; Becker, E. D. *J. Phys. Chem.* **1973**, *77*, 1783.
(3) Aksnes, D. W.; Kimtys, L. L. *Magn. Reson. Chem*. **1991**, *29*, 698.
(4) Szcześniak, E. *Mol. Phys.* **1986**, *4*, 679.
(5) Bakke, J. M. *Acta Chem. Scand. B* **1985**, *39*, 15.
(6) Woznyj, M.; Lang, E. W.; Lüdemann, H.-D. *J. Phys., Colloq.* **1984**, *C7*, 179.
(7) Fishman, E.; Drickamer, H. G. *J. Chem. Phys.* **1956**, *24*, 548.
(8) Fiorito, R. B.; Meister, R. *J. Chem. Phys.* **1972**, *56*, 4605.
(9) Marzke, R. F.; Raffaelle, D. P.; Halvorson, K. E.; Wolf, G. H. *J. Non-Cryst. Solids* **1994**, *172*−*174*, 401.
(10) Bull, T. E.; Jonas, J. *J. Chem. Phys.* **1970**, *52*, 4553.
(11) (a) Wallen, S. L.; Palmer, B. J.; Garrett, B. C.; Yonker, C. R. *J. Phys. Chem.* **1996**, *100*, 3959. (b) Ibid. **1996**, *100*, 20173.
(12) Jonas, J.; Akai, J. A. *J. Chem. Phys.* **1977**, *66*, 4946.
(13) Oldenziel, J. G.; Trappeniers, N. J. *Physica A* **1976**, *83*, 161.
(14) Aksnes, D. W.; Ramstad, K.; Bjorlykke, O. P. *Magn. Reson. Chem.* **1987**, *25*, 1063.
(15) Aksnes, D. W.; Ramstad, K. *Magn. Reson. Chem*. **1989**, *27*, 830.
(16) Margalit, Y. *J. Chem. Phys.* **1971**, *55*, 3072.
(17) Yonker, C. R.; Zemanian, T. S.; Wallen, S. L.; Linehan, J. C.; Franz, J. A. *J. Magn. Reson., Ser. A* **1995**, *113*, 102.
(18) Raynes, W. T.; Buckingham, A. D.; Bernstein, H. J. *J. Chem. Phys.* **1961**, *34*, 1084.
(19) Rummens, F. H. A.; Bernstein, H. J. *J. Chem. Phys.* **1965**, *43*, 2971.
(20) Buckingham, A. D. *Can. J. Chem.* **1960**, *38*, 300.
(21) Linowski, J. W.; Liu, N−I.; Jonas, J. *J. Magn. Reson.* **1976**, *23*, 455.
(22) Schulman, E. M.; Dwyer, D. W.; Doetschman, D. C. *J. Phys. Chem.* **1990**, *94*, 7308.
(23) Weast, D. C. *Handbook of Chemistry and Physics*, 77th ed.; CRC Press: Boca Raton, FL, 1996; pp 6−53.
(24) Albert, S.; Gutowsky, H. S.; Ripmeester, J. A. *J. Chem. Phys.* **1972**, *56*, 3672.
(25) Matsuo, S.; Makita, T. *Int. J. Thermophys.* **1991**, *12*, 459.
(26) Aksnes, D. W.; Kimtys, L. L. *Magn. Reson. Chem.* **1990**, *28*, 820.
(27) Feeney, J.; Walker, S. M. *J. Chem. Soc. A* **1966**, 1148.
(28) Davis, J. C.; Pitzer, K. S.; Rao, C. N. R. *J. Phys. Chem.* **1960**, *64*, 1744.
(29) Sweeting, L. M.; Becker, E. D. *J. Phys. Chem.* **1984**, *88*, 6075.
(30) Jorgensen, W. L. J. *Phys. Chem*. **1986**, 90, 1276.
(31) Jorgensen, W. L.; Madura, J. D.; Swenson, C. J. *J. Am. Chem. Soc*. **1984**, *106*, 6638.
(32) Wilhoit, R. C.; Zwolinski, B. J. *J. Phys. Chem. Ref. Data* **1973**, *2*, Suppl. 1, 1.
(33) Palmer, B. J.; Anchell, J. L. *J. Phys. Chem*. **1995**, *99*, 12239.
(34) Andersen, H. C. *J. Chem. Phys*. **1980**, *72*, 2384.
(35) Nosé, S. *J. Chem. Phys*. **1984**, *81*, 511.
(36) Palmer, B. J.; Garrett, B. C. *J. Chem. Phys*. **1993**, *98*, 4047.
(37) Israelachvili, J. *Intermolecular and Surface Forces*, 2nd ed.; Academic Press: New York, 1992.
(38) Jacobson, J.; Stockmayer, W. H. *J. Chem. Phys.* **1950**, *18*, 1600.
(39) Karmakar, A. K.; Sarkar, S.; Joarder, R. N. *J. Phys. Chem.* **1995**, *99*, 16501.